Eur J Nucl Med Mol Imaging (2008) 35:1147–1158
DOI 10.1007/s00259-007-0683-z

ORIGINAL ARTICLE

Ratio of dopamine synthesis capacity to D2 receptor availability in ventral striatum correlates with central processing of affective stimuli

Thorsten Kienast · Thomas Siessmeier · Jana Wrase · Dieter F. Braus · Michael N. Smolka · Hans Georg Buchholz · Michael Rapp · Mathias Schreckenberger · Frank Rösch · Paul Cumming · Gerhard Gruender · Karl Mann · Peter Bartenstein · Andreas Heinz

Received: 26 July 2007 / Accepted: 14 December 2007 / Published online: 17 January 2008

Abstract
Purpose Dopaminergic neurotransmission in the ventral striatum may interact with limbic processing of affective stimuli, whereas dorsal striatal dopaminergic neurotransmission can affect habitual processing of emotionally salient stimuli in the pre-frontal cortex. We investigated the dopaminergic neurotransmission in the ventral and dorsal striatum with respect to central processing of affective stimuli in healthy subjects.
Methods Subjects were investigated with positron emission tomography and [^{18}F]DOPA for measurements of dopamine synthesis capacity and [^{18}F]DMFP for estimation of dopamine D2 receptor binding potential. Functional magnetic resonance imaging was used to assess the blood-oxygen-level-dependent (BOLD) response to affective pictures, which was correlated with the ratio of [^{18}F]DOPA net influx constant K_{in}^{app}/[^{18}F]DMFP-binding potential (BP_ND) in the ventral and dorsal striatum.
Results The magnitude of the ratio in the *ventral* striatum was positively correlated with BOLD signal increases elicited by negative versus neutral pictures in the right medial frontal gyrus (BA10), right inferior parietal lobe and left post-central gyrus. In the *dorsal* striatum, the ratio was positively correlated with BOLD signal activation elicited

Thorsten Kienast and Thomas Siessmeier contributed equally to this work.

T. Kienast · J. Wrase · M. Rapp · A. Heinz (✉)
Department of Psychiatry and Psychotherapy of the Charité
University Medical Center, Charité Campus Mitte,
Charitéplatz 1,
10117 Berlin, Germany
e-mail: Andreas.Heinz@charite.de

F. Rösch
Institute of Nuclear Chemistry, University of Mainz,
Mainz, Germany

T. Siessmeier · H. G. Buchholz · M. Schreckenberger
Department of Nuclear Medicine, University of Mainz,
Mainz, Germany

P. Bartenstein
Department of Nuclear Medicine,
Ludwig-Maximilians-University,
Munich, Germany

D. F. Braus
Neuroimage Nord, Department of Psychiatry,
University of Hamburg,
Hamburg, Germany

J. Wrase · M. N. Smolka · K. Mann · A. Heinz
Central Institute of Mental Health,
Mannheim, Germany

P. Cumming
PET Center and Center for Functionally Integrative Neuroscience,
Aarhus, Denmark

G. Gruender
Department of Psychiatry of the RWTH,
Aachen University Medical Center,
Mainz, Germany

by negative versus neutral stimuli in the left post-central gyrus. The BOLD signal elicited by positive versus neutral stimuli in the superior parietal gyrus was positively correlated with the dorsal and ventral striatal ratio.

Conclusions The correlations of the ratio in the ventral and dorsal striatum with processing of affective stimuli in the named cortical regions support the hypothesis that dopamine transmission in functional divisions of the striatum modulates processing of affective stimuli in specific cortical areas.

Keywords Nucleus accumbens · Dopamine synthesis capacity · Dopamine D2 receptors · PET · fMRI

Introduction

Effects of dopamine on post-synaptic D2-like receptors may modulate the gating of sensory-, motor- and reinforcement-associated afferents that converge in the striatum [1–3]. Furthermore, dopaminergic neurotransmission in the ventral and dorsal striatum may differentially modify activity in cortico-striatal-thalamic circuits modulating the processing of salient environmental stimuli [4–6]. The ventral striatum, including the nucleus accumbens, has been identified as a key area for modulation of reward in humans [7–9] and also mediates negative reinforcement in response to aversive stimuli [10, 11]. Animal studies have shown that the ventral striatum receives direct projections from the pre-frontal and medial pre-frontal cortex and is consequently poised to modulate information processing in the dorsal striatum, which is anatomically closely associated with the dorsolateral pre-frontal cortex [12–15]. In the ventral striatum, dopaminergic neurotransmission interacts with the attentional and motivational response to reinforcing environmental stimuli, which is processed in the medial pre-frontal cortex, anterior cingulate and limbic cortices [12–15]. On the other hand, dopamine neurotransmission in the dorsal striatum may affect habitual processing of reinforcing stimuli in the dorsolateral pre-frontal cortex, thus, interacting with attention, executive control and reward learning [16–19].

Positron emission tomography (PET) technology enables the investigation of the brain dopamine system of living humans [20]. In humans, striatal uptake of the 3,4-dihydroxy-L-phenylalanine (DOPA) decarboxylase substrate 6-[^{18}F]fluoro-L-DOPA ([^{18}F]DOPA)-measured PET can be used as a surrogate marker for in vivo dopamine synthesis capacity [21]; as such, [^{18}F]DOPA trapping may be more indicative of tonic rather than phasic dopamine release [22, 18]. In a previous [^{18}F]DOPA–PET study, we observed that dopamine synthesis capacity in the ventral striatum correlated with the processing of affectively positive stimuli in the anterior cingulate and insula, whereas tracer uptake in the dorsal striatum correlated with processing of positive stimuli in the dorsolateral pre-frontal cortex [23]. Whereas [^{18}F]DOPA is a pre-synaptic tracer of dopamine innervations, the binding potential (BP_ND) of [^{18}F]DMFP and other ligands for dopamine D2 receptors are mainly sensitive to the availability of post-synaptic receptors. As these two tracers detect separate elements of dopamine neurotransmission [24], there is evidence that their ratio ([^{18}F]DOPA net influx /[^{18}F]DMFP BP_ND) may serve as a normalised indicator of net dopamine signalling in the living brain [25, 26].

To elucidate the association between dopamine D2 transmission in the ventral and dorsal striatum and central processing of emotionally salient stimuli, we used functional MRI (fMRI) to map blood oxygenation level-dependent (BOLD) signal changes evoked by standardised emotionally laden visual stimuli [27] in a group of subjects also investigated with [^{18}F]DOPA and [^{18}F]DMFP PET. Based on the results of our previous correlative imaging study [23] and on the neuroanatomical findings of Alexander and Crutcher [4] and Haber et al. [14, 15], we hypothesised that both the dopamine D2 receptor availability and the ratio of dopamine synthesis capacity to D2 receptor availability in the ventral striatum correlate with processing of affectively salient stimuli of positive and negative valence in the insula, in orbital and medial pre-frontal cortical brain areas. We also tested the hypothesis that, in the dorsal striatum, i.e. the central putamen and caudate, the magnitude of the two PET indices correlate with the processing of emotionally salient stimuli in the dorsolateral pre-frontal cortex, as revealed by BOLD signal changes evoked by visual stimuli with emotional content.

Materials and methods

Subjects and instruments

The local Ethics Committee approved the study, and written informed consent was obtained from all participants after the procedures had been fully explained. Twelve healthy men (mean age, 43.5±9.9; range, 32–60 years) were included. All three scans ([^{18}F]DOPA, [^{18}F]DMFP and fMRI) were performed within a period of 2 weeks. Random urine drug tests and standardised clinical assessment were performed to exclude axis I psychiatric disorders according to DSM IV and ICD (structured clinical interviews I and II) [28, 29].

General PET methods

Subjects were positioned in an ECAT EXACT PET scanner (Siemens Medical Solutions, Erlangen, Germany) so that the transaxial slices were parallel to the cantomeatal line.

The head of each subject was partially immobilised using polystyrene straps. For proper tissue attenuation correction, a 10-min transmission scan with a rotating external ^{68}Ge rod source was performed before [^{18}F]DOPA injection. Dynamic emission recordings were then acquired in 3D mode for both tracers. The emission sequences during a total of 124 min consisted of a series of 30 frames of the following dimension: 3×20 s, 3×1 min, 3×2 min, 3×3 min, 15×5 min, and 3×10 min. The subjects rested in the scanner with their eyes closed during the emission recording. After scanner-specific dead time and scatter correction, the data were reconstructed using filtered back projection (Hamming filter; width, 4 mm). The resulting images had a spatial axial resolution of 5.4 mm FWHM and 47 planes with a plane spacing of 3.375 mm and a pixel size of 2 mm (zoom factor, 2.5) within a matrix of 128×128 pixels. Before further data analysis, all PET dynamics were carefully checked for head movements and frame-by-frame motion corrected if necessary [30, 31].

Dopamine D2 receptor-binding potential measured by PET and [^{18}F]desmethoxyfallypride

We used PET and the benzamide radioligand [^{18}F]desmethoxyfallypride ([^{18}F]DMFP), which binds with intermediate affinity and high selectivity to D2-like dopamine receptors [30, 31]. PET data were acquired dynamically after administration of a mean of 194 MBq of [^{18}F]DMFP (SD=27). Specific activity at the time of injection was a mean of 267 GBq/μmol (range, 134–834 GBq/μmol), resulting in injected tracer masses of <1 μmol. We used a voxelwise simplified reference tissue model with the cerebellum serving as a reference region largely devoid of D2-like receptors [31, 32]. The calculated binding potential (BP_ND) is proportional to the ratio of B_{max} (the total concentration of specific binding sites) to K_d (the equilibrium dissociation constant), reduced to an unknown extent by competition from endogenous dopamine [33].

Dopamine synthesis capacity measured by PET and [^{18}F]DOPA

We used [^{18}F]DOPA PET to map the capacity for dopamine synthesis in the living brain by calculating the net blood–brain clearance of the tracer [34, 35]. To block extracerebral L-DOPA decarboxylase activity, all subjects were given carbidopa (2.5 mg/kg body weight) orally 60 min before scanning. The dynamic emission sequence was initiated after intravenous injection of [^{18}F]DOPA (mean, 194±27 MBq). A series of 40 arterial blood samples was collected at intervals during the emission recording, and the total radioactivity in plasma samples using a well-counter cross-calibrated to the PET. The fraction of untransformed [^{18}F]DOPA and the main plasma metabolite *O*-methyl-[^{18}F]DOPA (OMFD) were measured in plasma extracts by high-performance liquid chromatography (HPLC) at 5, 10, 15, 20, 30, 45, 60, 90, and 120 min post-injection by reversed phase HPLC using a Nucleosil 100 RP 18 column (250×4 mm), and the metabolite-corrected input calculated by bi-exponential fitting the measured fractions [36]. Based on the multiple time graphical analysis [37], the net blood–brain clearance of [^{18}F]DOPA from the plasma to the brain (K_{in}^{app}, ml g^{-1} min^{-1}) was calculated voxelwise by linear graphical analysis after subtracting the radioactivity measured in the cerebellum and using frames recorded in the interval 20–70 min p.i. for the linear analysis [21, 34, 35, 38]. This net blood–brain clearance is a macroparameter defined in terms of the unidirectional clearance of [^{18}F]DOPA from blood to brain (K_1^D; ml g^{-1} min^{-1}), the fractional rate constant for the transfer of tracer back to blood (k_2^D; min^{-1}), and the local activity of DOPA decarboxylase (k_3^D; min^{-1}). As such, the magnitude of K_{in}^{app} has the units of cerebral blood flow and reflects the local capacity in the brain parenchyma to form [^{18}F]fluorodopamine from plasma [^{18}F]DOPA and to retain that product within vesicles, mainly located in nigrostriatal nerve terminals. While widely accepted as a surrogate marker for the activity of DOPA-decarboxylase and, thus, interpreted as a reflection of dopamine synthesis capacity, the calculation of K_{in}^{app} is based upon a number of physiological assumptions, including those related to the subtraction of reference-region radioactivity, which is intended to correct for the presence in the brain of OMFD. Furthermore, it is assumed that the [^{18}F]fluorodopamine formed from [^{18}F]FDOPA is entirely retained within the brain during the recording interval of 70 min. A precise description of the [^{18}F]FDOPA kinetic modelling used in this study is discussed in literature [21, 36, 38].

Definition of regions of interest and [^{18}F]DOPA to [^{18}F]desmethoxyfallypride ratio

Regions of interest (ROIs) from individual subjects were defined on high-resolution MRI (T1-weighted image data sets acquired on a Siemens 1.5T Magnetom Vision MR tomography (Erlangen, Germany) using an MPRAGE sequence, 180 images in sagittal orientation with isotropic voxels of 1×1×1 mm^3).

The ventral striatum ROI was defined manually according to Mawlawi et al. [39] on coronal images (three adjacent planes). The ROIs for the dorsal striatum were drawn manually on transaxial images in the caudate and putamen (a total of six ROIs on three adjacent planes), excluding the most dorsal part of the putamen to minimise partial volume effects caused by the limited resolution of the PET images. Summed early emission frames of both

PET studies were co-registered to the individual T1-weighted MR images. After carefully inspecting the PET-to-common MR registrations, we resampled the individual native space [^{18}F]DMFP *BP_ND* or [^{18}F]DOPA K_{in}^{app} maps using the calculated transformation parameters. The ROIs were superimposed on the co-registered [^{18}F]DMFP BP_ND and [^{18}F]DOPA K_{in}^{app} maps. ROI statistics were performed, and the mean BP_ND and mean K_{in}^{app} for each ROI derived from unsmoothed PET data were extracted (Fig. 1). The magnitudes of BP_ND and K_{in}^{app} were averaged for VOIs from both hemispheres, resulting in one average value for the ventral striatum and one average value for the dorsal striatum. Finally, we calculated ratios of K_{in}^{app} to BP_ND from the ventral and dorsal striatum to normalise the amount of dopamine delivery to individual D2 receptor availability.

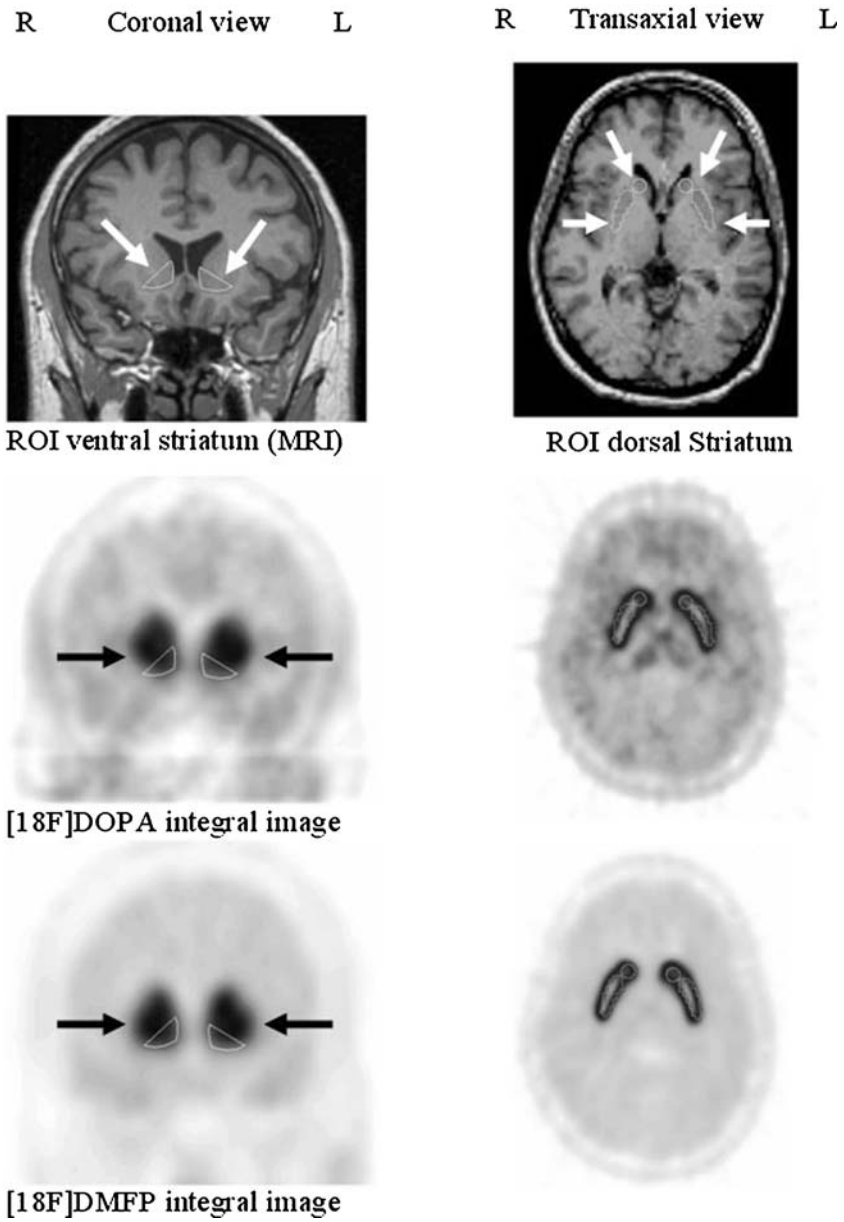

Fig. 1 *Left up* Coronal high resolution MRI with bilateral ventral striatal ROI defined according to Mawlawi et al. [39] (T1-weighted image, Siemens 1.5T Magnetom Vision MR tomograph, MP-RAGE sequence, isotropic voxels of 1×1×1 mm ROIs). *Left middle* For illustrative purposes, ROIs superimposed to an [18F]DOPA summation image. *Right middle* Transaxial view of the [18F]DOPA summation image illustrating the placement of the ROIs for caudate and putamen (dorsal striatum). *Left bottom* ROIs superimposed to an coronal [18F]DMFP summation image. *Right bottom* Transaxial view of the [18F]DMFP add image illustrating again the placement of the ROIs for caudate and putamen (all summation images were calculated for emission frames from 64 to 94 min post-injection)

Functional magnetic resonance imaging

To evoke emotional experience during the fMRI session, we used affectively negative, positive and neutral pictures taken from the International Affective Picture System (IAPS) [27]. These pictures have previously been shown to elicit significant fMRI activation in the pre-frontal and anterior cingulate cortices, as well as in the amygdala [24, 40, 41]. We first checked all pictures for arousal and valence using the standardised rating procedure described by Bradley and Lang [27]. Valence was rated on a scale from 1 (unhappy) to 9 (happy); positive pictures were rated 7.7±0.9, neutral pictures 5.8±1.1 and negative pictures 2.6±2.4. Arousal was rated on a scale from 1 (low) to 9 (high); positive pictures were rated 5.1±1.0, neutral pictures 2.7±1.4 and negative pictures 5.4±2.9. Subjects viewed the images passively [24, 40–42] in an event-related design for 750 ms; the pictures were arranged randomly for each subject.

Reconstructing the BOLD event-related time course requires sampling fMRI data at different peristimulus time points. This was achieved by random jitter between the inter-trial interval and the acquisition time, resulting in an equal distribution of data points after each stimulus. The inter-trial interval was randomised between three and six acquisition times (i.e. 9.9–19.8 s). During the inter-trial interval, a fixation condition was presented. FMRI scanning was performed with a 1.5 T clinical whole-body tomograph (Magnetom Vision; Siemens, Erlangen, Germany) equipped with a standard quadrature head coil, using the automatic Siemens MAP shim for shimming. For fMRI, 24 slices were acquired every 3.3 s (4-mm thickness, 1-mm gap) using a standard echo-planar imaging sequence (TR=1.8 ms, TE=66 ms, α=90°) with an in-plane resolution of 64×64 pixels (FOV 220 mm). FMRI slices were oriented axially parallel to the AC–PC line according to Talairach and Tournoux [43]. For anatomical reference, we acquired a morphological 3D T1-weighted magnetization-prepared rapid gradient echo (MPRAGE) image data set (1×1×1 mm^3 voxel size, FOV 256 mm, 162 slices, TR=11.4 ms, TE=4.4 ms, and α=12°) covering the whole head.

We used statistical parametric mapping (SPM5) to analyse fMRI data [44]. The structural 3D data set was co-registered to the first T2* image and the structural image spatially normalised to a standard template using a 12-parameter affine transformation with additional non-linear components. A non-linear transformation was subsequently applied to the T2* data. The functional data were smoothed using an isotropic Gaussian kernel for group analysis (12 mm FWHM). In our statistical analysis, we used SPM5 to model the different conditions (positive, negative, and neutral pictures; delta functions convolved with a synthetic hemodynamic response function and its time derivative) on a voxel-by-voxel basis as explanatory variables within the context of the general linear model (GLM). We analysed data for each subject individually (threshold, $p<0.001$, uncorrected). To detect differences in the BOLD response elicited by emotional stimuli, we included the contrast images (signal change of positive versus neutral and negative versus neutral pictures) of all subjects in a second-level random effects analysis.

Statistical analysis of correlations between the central processing of affective stimuli and [^{18}F]DOPA K_{in}^{app}/[^{18}F]DMFP (BP_ND) ratio

To detect the association between voxelwise changes in BOLD signal and both striatal [^{18}F]DMFP BP_ND and the [^{18}F]DOPA K_{in}^{app}/[^{18}F]DMFP (*BP_ND*) ratio, we included the contrast images of all subjects in a second-level regression analysis with SPM5. In the confirmatory part of the analysis, we tested the hypotheses that (1) the magnitudes of D2 BP_ND and the K_{in}^{app}/*BP_ND* binding ratio in the ventral striatum correlate with the processing of emotional stimuli in parts of the pre-frontal and limbic cortex with direct projections to the ventral striatum and (2) that the D2 BP_ND and the K_{in}^{app}/*BP_ND* binding ratio in the dorsal striatum correlate with the processing of emotional stimuli in the dorsolateral pre-frontal cortex [4, 14, 15]. In the exploratory part of the analysis, we assessed whether the DMFP BP_ND or the [^{18}F]DOPA K_{in}^{app}/[^{18}F]DMFP (*BP_ND*) ratio is associated with functional activation in further brain areas that were significantly activated by affective versus neutral stimuli but which have no known direct anatomical connection with the ventral or dorsal striatum [4, 14]. A significance level of $p<0.001$ uncorrected was chosen for all correlational analyses.

Results

Results for [^{18}F]DMFP-binding potential and [^{18}F]DOPA uptake PET measures

The mean magnitude of the [^{18}F]DMFP *BP_ND* among the 12 subjects was 1.84±0.31 in the bilateral ventral striatum and 2.37±0.40 in the bilateral dorsal striatum. The magnitudes of [^{18}F]DMFP BP_ND in the ventral and dorsal striatum were significantly correlated (Pearson's R=0.96, $p<0.001$).

The mean magnitude of the [^{18}F]DOPA K_{in}^{app} was 0.0090±0.0022 ml g^{-1} min^{-1} in the bilateral ventral striatum and 0.0118±0.0027 ml g^{-1} min^{-1} in the bilateral dorsal striatum. The magnitudes of [^{18}F]DOPA K_{in}^{app} in the ventral and dorsal striatum were significantly correlated (Pearson's R=0.94, $p<0.001$).

Striatal [^{18}F]DOPA net blood brain influx K_{in}^{app} was not significantly correlated with [^{18}F]DMFP BP_ND: We ob-

served neither a significant correlation in the ventral (R=0.02, p=0.47) nor dorsal striatum (R=0.24, p=0.22).

The mean magnitude of the *ratio* K_{in}^{app}/BP_ND was 0.0050±0.0015 in the ventral striatum and 0.0051±0.0015 in the dorsal striatum (Fig. 1). The K_{in}^{app}/*BP_ND* ratios in the ventral and dorsal striatum were positively correlated (Pearson's R=0.92, p=0.001).

FMRI BOLD contrast and its correlation with [^{18}F]DOPA K_{in}^{app}/[^{18}F]DMFP (BP_ND) ratio

Similar to previous studies [23, 40, 41], the presentation of affective vs neutral pictures elicited significant BOLD contrasts in the limbic [left parahippocampal gyrus (BA 34) and left anterior cingulate cortex (BA 24)], frontal (right BA 6, BA 10 and BA 46), parietal (right BA 40), temporal (left BA 37 and BA 39) and occipital cortex (bilateral BA 19), as well as in the right mamillary body and right hypothalamus (Table 1).

The [^{18}F]DMFP *BP_ND* was not significantly correlated with the fMRI BOLD response elicited by affective stimuli, neither in brain areas directly connected with the ventral or dorsal striatum nor in any other brain area that showed a significant activation elicited by affective versus neutral stimuli (data not shown).

Correlations between the K_{in}^{app}/BP_ND ratio in the ventral striatum and functional activation elicited by affective stimuli

In accordance with our hypothesis, the magnitude of the K_{in}^{app}/*BP_ND* ratio in the ventral striatum was positively correlated with the BOLD response elicited by *negative versus neutral stimuli* in the right medial frontal gyrus (BA 10, *x*/*y*/*z*=21/50/9, T=4.73, R=0.83, cluster size=15 voxel, p<0.001; Table 2, negative versus neutral pictures; Fig. 2).

Exploratory analysis revealed that the ventral striatal K_{in}^{app}/*BP_ND* ratio was also positively correlated with the fMRI BOLD response elicited by *negative versus neutral* stimuli in the right inferior parietal lobe (BA 5, *x*/*y*/*z*=42/−44/58, T=6.37, R=0.90, cluster size=86 voxel, p<0.001; Table 2, negative versus neutral pictures) and in the left post-central gyrus (BA 2, *x*/*y*/*z*=−39/−38/63, T=9.46, R=0.95, cluster size=27 voxel, p<0.001; Table 2, negative versus neutral pictures; Fig. 3a).

Exploratory analysis also revealed that the ventral striatal K_{in}^{app}/*BP_ND* ratio was positively correlated with the fMRI BOLD response elicited by *positive versus neutral* stimuli in the left superior parietal lobule (BA 7, *x*/*y*/*z*=−24/−46/63, T=5.45, R=0.87, p<0.001; Table 2, positive versus neutral pictures; Fig. 3b).

Correlations between the K_{in}^{app}/BP_ND ratio in the bilateral dorsal striatum and functional activation elicited by affective visual stimuli

There was no finding in accordance with our hypothesis.

Exploratory analysis revealed that the magnitude of the K_{in}^{app}/*BP_ND* ratio was positively correlated with the BOLD response elicited by *negative versus neutral stimuli* in the left post-central gyrus (BA 2, *x*/*y*/*z*=−33/−38/65, T=6.17, R=0.89, cluster size=16, p<0.001; Table 3, negative versus neutral pictures; Fig. 3c).

Table 1 FMRI BOLD response contrast elicited by positive and negative versus neutral affective visual stimuli in 12 healthy male volunteers at p<0.001 uncorrected

Lobe	Location	BA	Side	Talairach			T	p Value	Cluster size (voxel)
				Coordinates					
				X	*y*	*z*			
Positive correlation									
Frontal	Inferior frontal gyrus	46	Right	56	32	7	4.71	<0.000	21
Parietal	Supramarginal gyrus	40	Right	56	−54	33	4.23	<0.001	2
Temporal	Middle temporal gyrus	39	Left	−48	−72	17	4.66	<0.000	21
Temporal	Middle temporal gyrus	37	Left	−56	−64	9	4.61	<0.000	21
Limbic	Parahippocampus	34	Left	−12	−10	−15	4.93	<0.000	11
Limbic	Anterior cingulated	24	Left	−1	32	−2	4.12	<0.001	4
Occipital	Lingual gyrus	19	Right	12	−61	−2	4.12	<0.001	1
Occioital	Cuneus	19	Left	−3	−86	32	4.61	<0.000	14
Frontal	Middle frontal gyrus	10	Right	33	47	12	4.58	<0.000	4
Frontal	Superior frontal gyrus	6	Right	21	3	63	5.11	<0.000	10
	Mamillary body		Right	12	−17	1	4.11	<0.001	1
	Hypothalamus		Right	1	−6	−10	4.04	<0.001	2

Table 2 Correlations between [^{18}F]DOPA K_{in}^{app}/[^{18}F]DMFP *(BP_ND)* in the ventral striatum and fMRI BOLD response elicited by affective visual stimuli in 12 healthy male volunteers at $p<0.001$

Lobe	Location	BA	Side	Talairach			*T*	*p* Value	Cluster size (voxel)
				Coordinates					
				x	*y*	*z*			
Negative versus neutral pictures: Positive correlation									
Frontal	Medial frontal gyrus	10	Right	21	50	9	4.73	<0.001	15
Parietal	Inferior parietal lobe	5	Right	42	−44	58	6.37	<0.001	86
Parietal	Post-central gyrus	2	Left	−39	−38	63	9.46	<0.001	27
No significant negative correlation									
Positive versus neutral pictures: Positive correlation									
Parietal	Superior parietal lobule	7	Left	−24	−46	63	5.45	<0.001	16
No significant negative correlation									

[18F]DMFP [18F] desmethoxyfallypride, K_{in}^{app} net influx of [^{18}F]DOPA from plasma to brain, *BP_ND* binding potential non-displacable, *fMRI* functional magnetic resonance imaging, *BOLD* blood oxygen level dependent

Exploratory analysis also showed that the K_{in}^{app}/*BP_ND* ratio in the bilateral dorsal striatum was positively correlated with the BOLD response elicited by *positive versus neutral stimuli* in the left superior parietal lobule (BA 7, *x*/*y*/*z*=−24/−46/63, *T*=7.06, *R*=0.91, cluster size=15 voxel, $p<0.001$; Table 3, positive versus neutral pictures; Fig. 3d).

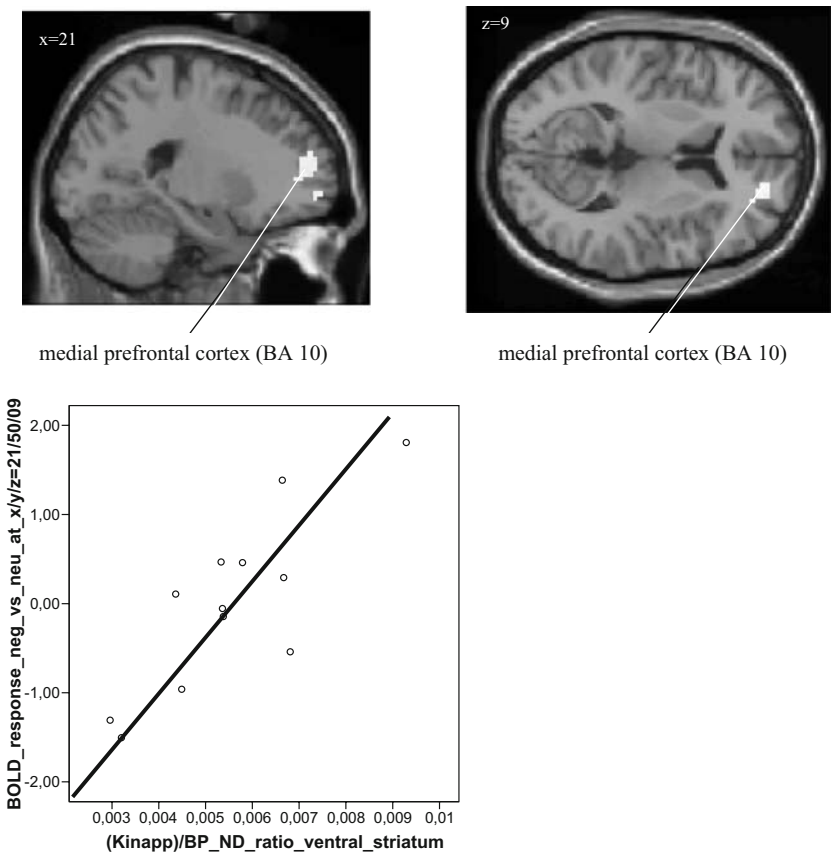

Fig. 2 *Upper half* Positive correlation between the magnitude of the ratio [^{18}F]DOPA K_{in}^{app}/[18F]DMFP (BP_ND) ratio in the bilateral ventral striatum and the BOLD response elicited by affectively negative versus neutral stimuli in the right medial pre-frontal cortex (BA 10), a brain area with evidence for anatomical linkage with the ventral striatum. For illustration purposes, image at significance level $p=0.002$ uncorrected. *Lower half* Plot of the correlation between the magnitude of the [^{18}F]DOPA K_{in}^{app}/[18F]DMFP (BP_ND) ratio in the bilateral ventral striatum and the BOLD response elicited by negative versus neutral stimuli in the right medial pre-frontal cortex in the peak voxel of the cluster (*x*/*y*/*z*=21/50/9, BA 10; *R*=0.83)

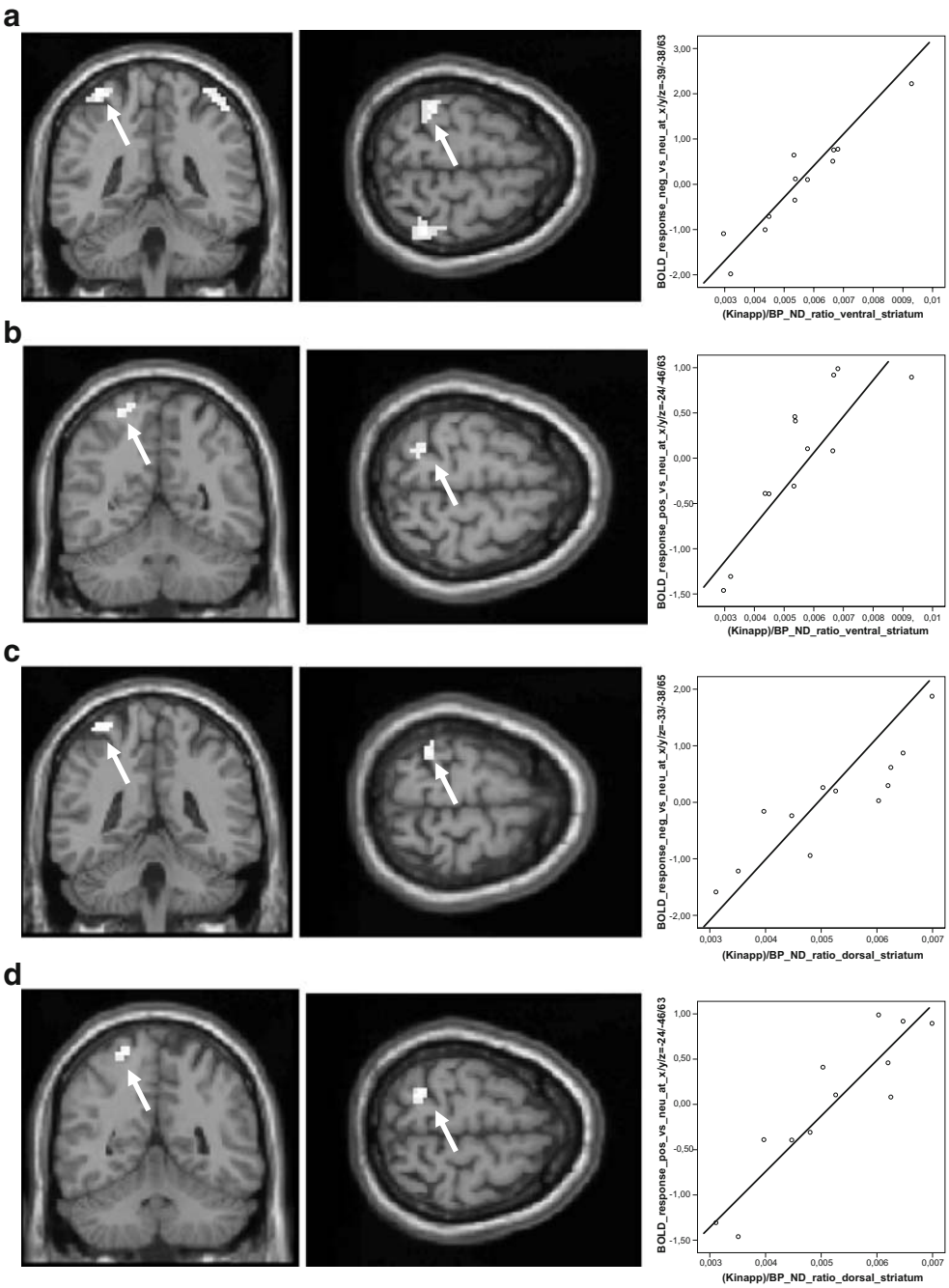

Fig. 3 Positive correlations between the magnitude of the ratio [^{18}F]DOPA K_{in}^{app}/[18F]DMFP (BP_ND) ratio in the bilateral ventral or dorsal striatum and the BOLD response elicited by affectively negative versus neutral or positive versus neutral stimuli. Images at significance level $p<0.001$. **a** At $x/y/z=-39/-38/63$. *Arrows* indicate left BA7 as reported in Table 2 (negative versus neutral pictures); correlation, $R=0.95$ and $p<0.001$. **b** At $x/y/z=-24/-46/63$. *Arrows* indicate left BA7 as reported in Table 2 (positive versus neutral pictures); correlation, $R=0.87$ and $p<0.001$. **c** At $x/y/z=-33/-38/65$. *Arrows* indicate left BA2 as reported in Table 3 (negative versus neutral pictures); correlation, $R=0.89$ and $p<0.001$. **d** At $x/y/z=-24/-46/63$. *Arrows* indicate left BA7 as reported in Table 3 (positive versus neutral pictures); correlation, $R=0.91$ and $p<0.001$

Discussion

In this study, we assessed the interaction between functional brain activation elicited by affective stimuli, and (1) striatal dopamine D2 receptor availability and (2) the ratio of dopamine synthesis capacity to local dopamine D2 receptor availability K_{in}^{app}/BP_ND. K_{in}^{app} is a parameter measured by PET standing for the net blood–brain clearance, which is interpreted as reflecting "dopamine synthesis capacity" [21, 38]. Very few PET studies report the assessment of pre- and post-synaptic dopaminergic parameters in the same subjects, and there is some evidence for the occurrence of a functional relation of dopamine D2 receptor availability and dopamine release, at least in alcoholic subjects [45]. In this study and in a previous study [24], the magnitudes of [^{18}F]DOPA K_{in}^{app} and [^{18}F]DMFP *BP_ND* were not significantly correlated; their ratio K_{in}^{app}/BP_ND was used to assess dopamine synthesis capacity relative to the local D2 receptor availability. Contrary to the hypothesis stated above, the local magnitude of [^{18}F]DMFP *BP_ND* did not significantly interact with central processing of emotional pictures, indicating that this parameter alone may be insufficient to characterise dopaminergic neurotransmission

Table 3 Correlation between [^{18}F]DOPA K_{in}^{app}/[^{18}F]DMFP *(BP_ND)* measures in the dorsal striatum and fMRI bold response elicited by affective visual stimuli in 12 healthy men at $p<0.001$

Lobe	Location	BA	Side	Talairach			T	p Value	Cluster size (voxel)
				Coordinates					
				x	y	z			
Negative versus neutral pictures: Positive correlation									
Parietal	Postcentral gyrus	2	Left	−33	−38	65	6.17	<0.001	16
No significant negative correlation									
Positive versus neutral pictures: Positive correlation									
Parietal	Superior parietal lobule	7	Left	−24	−46	63	7.06	<0.001	15
No significant negative correlation									

[18F]DMFP [18F] desmethoxyfallypride, K_{in}^{app} net influx of [^{18}F]DOPA from plasma to brain, *BP_ND* binding potential non-displacable, *fMRI* functional magnetic resonance imaging, *BOLD* blood oxygen level dependent

in the ventral or dorsal striatum. However, when the index *BP_ND* was used to "normalise" dopamine synthesis capacity to local D2 receptor availability [25, 26], we observed significant interactions between the magnitude of the calculated K_{in}^{app}/*BP_ND* ratio and the processing of emotionally aversive and positive stimuli in brain areas with direct or a high likelihood for anatomical connections to the ventral and dorsal striatum. Therefore, we propose this ratio as an index of dopamine synthesis capacity normalised to the local availability of dopamine D2-like receptors. The magnitude of K_{in}^{app}/*BP_ND* may reflect tonic rather than phasic dopaminergic neurotransmission proposed on the basis of the electrophysiology of dopamine neurons [22], in that dopamine synthesis may be affected by the prevailing occupancy of dopamine D2 (auto) receptors in the basal ganglia. In the cerebral cortex, high tonic dopamine neurotransmission may be associated with increased cortical dopamine D1 receptor stimulation and a sustained execution of pre-potent response sets [18].

We and others have previously shown that the presentation of affective versus neutral stimuli activates a distributed network of brain areas including the frontal (e.g. BA 10), limbic (e.g. anterior cingulate), temporal, parietal and occipital cortex [23, 40, 41, 46]. As previously described by Phan et al. [46] and Wrase et al. [40], brain areas activated by positive versus neutral stimuli differed from those activated by negative versus neutral pictures, which may indicate processing of different emotions in separate networks. In accordance with our hypothesis, the magnitude of K_{in}^{app}/*BP_ND* in the ventral striatum was significantly correlated with processing of emotionally aversive cues in the medial pre-frontal cortex (BA 10). Confirming the results of anatomical studies in animal experiments, our results suggest the medial frontal cortex to be not only anatomically [12–15, 47, 48] but also functionally connected to the ventral striatum. The BA 10 is known to be involved in attentional processing and memory retrieval [49–51].

In the exploratory analysis, we also observed that, in the ventral and dorsal striatum, the magnitude of the K_{in}^{app}/*BP_ND* ratio was positively correlated with processing of *aversive* stimuli in the left post-central gyrus (BA 2) and, for the ventral striatum, also in the right inferior parietal lobe (BA 5). Moreover, BOLD signal changes in the left superior parietal lobule (BA 7) during the processing of *positive* pictures were correlated with the ratio K_{in}^{app}/*BP_ND* in both ventral and dorsal striatum. Previous anatomical studies have revealed direct fiber projections from BA 2 and 5 (or analogous regions in the primate) to ventral and dorsal striatum in primates [52–55]. Functionally, the pre-central cortex and the superior and inferior parietal lobe (BA 2, BA 5 and BA 7) are known to be involved in complex sensory-motor processing such as somatosensory feedback and integration procedures, as well as in execution and motor imagery learning, motor attention and in the preparation and redirection of movements and movement intentions [56, 57, 58].

Dopamine synthesis capacity K_{in}^{app} was not significantly correlated with [^{18}F]DMFP BP_ND in the ventral or dorsal striatum. In a comparable study by Volkow et al. [59], DAT and D2 receptor availability were significantly correlated, which may point to a functional coupling between dopamine reuptake (which directly influences extracelluar dopamine concentrations) and D2 receptor availability. Dopamine synthesis capacity on the other hand will influence intrasynaptic dopamine concentrations depending on neuronal activity (action potential, dopamine release) and may be leakage from pre-synaptic dopamine neurons [60]. Technical limitations of both PET methods may also contribute to this lack of correlation in our study. On the other hand, PET measures in the ventral striatum for each method were significantly correlated with the same measure

in the dorsal striatum, most likely caused by potential cross-talking (see limitations below).

Several limitations of the present study need to be addressed. First, the sample size was limited, and only male subjects were examined to avoid confounding of results by gender differences in the processing of affective stimuli [40, 61]. With respect to this limited sample size and the explorative nature of the study, we chose a rather liberal statistical significance level ($p<0.001$ uncorrected at the voxel level) without correction for multiple testing, e.g. with regional masks. However, as our results complement findings of anatomical studies [4, 14], we feel that the observed correlations may reflect valid functional interactions. Second, the present correlational analysis does not indicate causality, and we do not know if dopamine transmission in the extended striatum drives the frontal cortex or vice versa. For example, the correlations between striatal measures of dopaminergic neurotransmission and functional brain activation observed in this study and in comparable studies of Meyer-Lindenberg et al. [62, 63] may indicate that individual differences in striatal and cortical dopamine tone are in some way related. Furthermore, the [^{18}F]DOPA K_{in}^{app} is only a surrogate marker for the unknown rate of dopamine synthesis in the living brain [21], as it is defined as a net influx of [^{18}F]DOPA from blood to brain. As such, the magnitude of K_{in}^{app} corresponds to the capacity of the brain to utilise [^{18}F]DOPA, which is indicative of the local activity of DOPA decarboxylase. However, the inherent rate of dopamine synthesis in the living human brain cannot be measured by PET, as the levodopa concentration in the brain is unknown. Finally, there was a rather high correlation between the magnitudes of the K_{in}^{app}*/BP_ND ratio* ($R=0.92$) in the dorsal and in the ventral striatum. Potential cross-talk between the dorsal and ventral striatum because of partial volume effects in D2 receptor PET scanning is well-known as a factor contributing to this high correlation. Mawlawi and coworkers suggested that even under rather optimal conditions, there is a 12–18% signal from the dorsal striatum present in the ventral and vice versa [39]. Indeed, correlations in our study were rather high between the ventral and dorsal striatum for both [^{18}F]DOPA uptake ($R=0.94$) and D2 availability ($R=0.96$), indicating that differences between ventral and dorsal striatum effects may be underestimated in our study. Further studies with larger sample sizes or employing a psychostimulant activation paradigm may help to further elucidate functional connections between dopaminergic neurotransmission in the ventral versus dorsal striatum and pre-frontal and limbic processing of salient stimuli.

In summary, we have used the magnitude of the ratio of [^{18}F]DOPA net influx to dopamine D2 receptor availability as an index of dopamine neurotransmission in striatum and tested the correlation between this index and the processing of emotionally laden images. Observing significant correlations between this ratio and anatomically closely connected brain areas supports the usefulness of this index of DA neurotransmission. Furthermore, the present findings strengthen the hypothesis that dopaminergic neurotransmission in the ventral versus dorsal striatum interacts with central processing of affective stimuli in separate fronto-striatal-thalamic circuits [4, 14].

Acknowledgment This study was supported by the Deutsche Forschungsgemeinschaft (HE 2597/4-3 and 2597/7-3). We thank Dr. Y. Kumakura for his help with data analysis.

References

1. Contreras-Vidal JL, Schultz W. A predictive reinforcement model of dopamine neurons for learning approach behavior. J Comput Neurosci. 1999;6:191–214.
2. Horvitz JC. Dopamine gating of glutamatergic sensorimotor and incentive motivational input signals to the striatum. Behav Brain Res. 2002;137:65–74.
3. Vollm BA, De Araujo IE, Cowen PJ, Rolls ET, Kringelbach ML, Smith KA, et al. Methamphetamine activates reward circuitry in drug naive human subjects. Neuropsychopharmacology 2004;29:1715–22.
4. Alexander GE, Crutcher MD. Functional architecture of basal ganglia circuits: neural substrates of parallel processing. Trends Neurosci. 1990;13:266–71.
5. Cummings JL. On frontal-subcortical circuits and human behavior. J Psychosom Res. 1998;44:627–8.
6. O'Reilly RC, Noelle DC, Braver TS, Cohen JD. Prefrontal cortex and dynamic categorization tasks: representational organization and neuromodulatory control. Cereb Cortex. 2002;12:246–57.
7. Breiter HC, Gollub RL, Weisskoff RM, Kennedy DN, Makris N, Berke JD, et al. Acute effects of cocaine on human brain activity and emotion. Neuron 1997;19:591–611.
8. Everitt BJ, Wolf ME. Psychomotor stimulant addiction: a neural systems perspective. J Neurosci. 2002;22:3312–20.
9. Schultz W. Behavioral theories and the neurophysiology of reward. Annu Rev Psychol. 2006;57:87–115.
10. Yasoshima Y, Scott TR, Yamamoto T. Memory-dependent c-Fos expression in the nucleus accumbens and extended amygdala following the expression of a conditioned taste aversive in the rat. Neuroscience. 2006;141:35–45.
11. Reynolds SM, Berridge KC. Positive and negative motivation in nucleus accumbens shell: bivalent rostrocaudal gradients for GABA-elicited eating, taste "liking"/"disliking" reactions, place preference/avoidance, and fear. J Neurosci. 2002;22:7308–20.
12. Ferry AT, Ongur D, An X, Price JL. Prefrontal cortical projections to the striatum in macaque monkeys: evidence for an organization related to prefrontal networks. J Comp Neurol 2000;425:447–70.
13. Ding DC, Gabbott PL, Totterdell S. Differences in the laminar origin of projections from the medial prefrontal cortex to the nucleus accumbens shell and core regions in the rat. Brain Res. 2001;917:81–9.
14. Haber SN, Fudge JL, McFarland NR. Striatonigrostriatal pathways in primates form an ascending spiral from the shell to the dorsolateral striatum. J Neurosci. 2000;20:2369–82.
15. Haber SN, Kim KS, Mailly P, Calzavara R. Reward-related cortical inputs define a large striatal region in primates that interface with

associative cortical connections, providing a substrate for incentive-based learning. J Neurosci. 2006;26:8368–76.
16. Wickens JR, Reynolds JNJ, Hyland BI. Neural mechanisms of reward-related motor learning. Curr Opin Neurobiol. 2003;13:685–90.
17. Kelly AM, Hester R, Murphy K, Javitt DC, Foxe JJ, Garavan Z. Prefrontal-subcortical dissociations underlying inhibitory control revealed by event-related fMRI. Eur J Neurosci. 2004;19:3105–12.
18. Bilder RM, Volavka J, Lachman HM, Grace AA. The catechol-*O*-methyltransferase polymorphism: relations to the tonic-phasic dopamine hypothesis and neuropsychiatric phenotypes. Neuropsychopharmacology. 2004;29:1943–61.
19. Christakou A, Robbins TW, Everitt BJ. Prolonged neglect following unilateral disruption of a prefrontal cortical-dorsal striatal system. Eur J Neurosci. 2005;21:782–92.
20. Volkow ND, Fowler JS, Gatley SJ, Logan J, Wang GJ, Ding YS, et al. PET evaluation of the dopamine system of the human brain. J Nucl Med. 1996;37:1242–56.
21. Cumming P, Gjedde A. Compartmental analysis of L-DOPA decarboxylation in living brain from dynamic positron emission tomograms. Synapse. 1998;29:37–61.
22. Grace AA. Phasic versus tonic dopamine release and the modulation of dopamine system responsivity: a hypothesis for the etiology of schizophrenia. Neuroscience 1991;41:1–24.
23. Siessmeier T, Kienast T, Wrase J, Larssen JL, Braus DF, Smolka MN, et al. Net influx of plasma 6-[^{18}F]fluoro-L-DOPA (FDOPA) to the ventral striatum correlates with prefrontal processing of affective stimuli. Eur J Neurosci. 2006;24:305–13.
24. Heinz A, Siessmeier T, Wrase J, Buchholz HG, Grunder G, Kumakura Y, et al. Correlation of alcohol craving with striatal dopamine synthesis capacity and D2/3 receptor availability: a combined [18F]DOPA and [18F]DMFP PET study in detoxified alcoholic patients. Am J Psychiatry. 2005;162:1515–20.
25. Laakso A, Pohjalainen T, Bergman J, Kajander J, Haaparanta M, Solin O, et al. The A1 allele of the human D2 dopamine receptor gene is associated with increased activity of striatal L-amino acid decarboxylase in healthy subjects. Pharmacogenet Genomics. 2005;15:387–91.
26. Antonini A, Vontobel P, Psylla M, Gunther I, Maguire PR, Missimer J, et al. Complementary positron emission tomographic studies of the striatal dopaminergic system in Parkinson's disease. Arch Neurol. 1995;52:1183–90.
27. Bradley MM, Lang PJ. Measuring emotion: the self-assessment manikin and the semantic differential. J Behav Ther Exp Psychiatry 1994;25:715–20.
28. First MB, Spitzer RL, Gibbon M, Williams J. Structured clinical interview for DSM-IV personality disorders, (SCID-II). Washington, DC: American Psychiatric Press; 1997.
29. First MB, Spitzer RL, Gibbon M, Williams J. Structured clinical interview for DSM-IV-TR Axis I disorders, research version, patient edition with psychotic screen (SCID-I/P W/ PSY SCREEN). New York: New York State Psychiatric Institute, Biometrics Research; 2001.
30. Gruender G, Siessmeier T, Piel M, Vernaleken I, Buchholz HG, Zhou Y, et al. Quantification of D2-like dopamine receptors in the human brain with [^{18}F]desmethoxyfallypride. J Nucl Med. 2003;44:109–16.
31. Siessmeier T, Zhou Y, Buchholz HG, Landvogt C, Vernaleken I, Piel M, et al. Parametric mapping of binding in human brain of D2 receptor ligands of different affinities. J Nucl Med. 2005; 46:964–72.
32. Gunn RN, Lammertsma AA, Hume SP, Cunningham VJ. Parametric imaging of ligand-receptor binding in PET using a simplified reference region model. Neuroimage 1997;6:279–87.
33. Laruelle M. Imaging synaptic neurotransmission with in vivo binding competition techniques: a critical review. J Cereb Blood Flow Metab. 2000;20:423–51.
34. Gjedde A. Exchange diffusion of large neutral amino acids between blood and brain. In: Rakic L et al., editor. Peptide and amino acid transport mechanisms in the central nervous system. New York: Stockton; 1988. p. 209–17.
35. Martin WR, Palmer MR, Patlak CS, Calne DB. Nigrostriatal function in humans studies with positron emission tomography. Ann Neurol. 1989;26:535–42.
36. Gillings NM, Bender D, Falborg L, Marthi K, Munk OL, Cumming P. Kinetics of the metabolism of four PET radioligands in living minipigs. Nucl Med Biol. 2001;28:97–104.
37. Patlak CS, Blasberg RG. Graphical evaluation of blood-to-brain transfer constants from multiple-time uptake data generalizations. J Cereb Blood Flow Metab 1985;5:584–90.
38. Kumakura Y, Danielsen EH, Reilhac A, Gjedde A, Cumming P. The influx of [^{18}F] fluorodopa to brain of normal volunteers and patients with Parkinson's disease: effect of levodopa. Acta Neurol Scand. 2004;110:188–95.
39. Mawlawi O, Martinez D, Slifstein M, Broft A, Chatterjee R, Hwang DR. Imaging human mesolimbic dopamine transmission with positron emission tomography, I: accuracy and precision of D(2) receptor parameter measurements in ventral striatum. J Cereb Blood Flow Metab. 2001;21:1034–57.
40. Wrase J, Klein S, Gruesser SM, Hermann D, Flor H, Mann K, et al. Gender differences in the processing of standardized emotional visual stimuli in humans: a functional magnetic resonance imaging study. Neurosci Lett. 2003;348:41–5.
41. Smolka MN, Schumann G, Wrase J, Grusser SM, Flor H, Mann K, et al. Catechol-*O*-methyltransferase val(158)met genotype affects processing of emotional stimuli in the amygdala and prefrontal cortex. J Neurosci. 2005;25:836–42.
42. Taylor SF, Phan KL, Decker LR, Liberzon I. Subjective rating of emotionally salient stimuli modulates neural activity. Neuroimage 2003;18:650–9.
43. Talairach J, Tournoux P. Co-planar stereotaxic atlas of the human brain 3-dimensional proportional system. An approach to cerebral imaging. Stuttgart, New York: Thieme; 1988.
44. Friston K.J, et al. London, UK. Wellcome Department of Imaging Neuroscience. 2005. http://www.fil.ion.ucl.ac.uk/spm/.
45. Volkow ND, Fowler JS, Wang GJ, Swanson JM. Dopamine in drug abuse and addiction. Results from imaging studies and treatment implications. Mol Psychiatry 2004;9:557–69.
46. Phan KL, Wager TD, Taylor SF, Liberzon I. Functional neuroimaging studies of human emotions. CNS Spectr 2004;9:258–66.
47. Gorelova N, Yang CR. The course of neural projection from the prefrontal cortex to the nucleus accumbens in the rat. Neuroscience 1997;76:689–706.
48. Arvanitogiannis A, Tzschentke TM, Riscaldino L, Wise RA, Shizgal P. Fos expression following self-stimulation of the medial prefrontal cortex. Behav Brain Res. 2000;107:123–32.
49. Burgess PW, Scott SK, Frith CD. The role of the rostral frontal cortex (area 10) in prospective memory: a lateral versus medial dissociation. Neuropsychologia 2003;41:906–18.
50. Heinz A, Siessmeier T, Wrase J, Hermann D, Klein S, Grusser SM, et al. Correlation between dopamine D(2) receptors in the ventral striatum and central processing of alcohol cues and craving. Am J Psychiatry 2004;161:1783–9.
51. Fuster JM. The prefrontal cortex: anatomy, physiology and neurophysiology of the frontal lobe. Philadelphia: Lippincott–Raven; 1997. p. 175–6.
52. Selemon LD, Goldman-Rakic PS. Common cortical and subcortical targets of the dorsolateral prefrontal and posterior parietal cortices in the rhesus monkey: evidence for a distributed neural network subserving spatially guided behavior. J Neurosci. 1988;8:4049–68.
53. Cavada C, Goldman-Rakic PS. Topographic segregation of corticostriatal projections from posterior parietal subdivisions in the macaque monkey. Neuroscience 1991;42:683–96.

54. Yeterian EH, Pandya DN. Striatal connections of the parietal association cortices in rhesus monkeys. J Comp Neurol. 1993;332:175–97.
55. Kunzle H. Projections from the primary somatosensory cortex to basal ganglia and thalamus in the monkey. Exp Brain Res. 1977;30:481–92.
56. Rushworth MF, Johansen-Berg H, Gobel SM, Devlin JT. The left parietal and premotor cortices: motor attention and selection. Neuroimage 2003;20(Suppl 1):S89–100.
57. Lacourse MG, Orr EL, Cramer SC, Cohen MJ. Brain activation during execution and motor imagery of novel and skilled sequential hand movements. Neuroimage 2005;27:505–19.
58. Hoffer ZS, Arantes HB, Roth RL, Alloway KD. Functional circuits mediating sensorimotor integration: quantitative comparisons of projections from rodent barrel cortex to primary motor cortex, neostriatum, superior colliculus, and the pons. J Comp Neurol. 2005;488:82–100.
59. Volkow ND, Wang GJ, Fowler JS, Logan J, Franceschi D, Maynard L, et al. Relationship between blockade of dopamine transporters by oral methylphenidate and the increases in extracellular dopamine: therapeutic implications. Synapse 2002; 43:181–7.
60. Grace AA. The tonic/phasic model of dopamine system regulation: its relevance for understanding alcohol and psychostimulant craving. Addiction 2000;95(Suppl 2):S119–28.
61. Canli T, Desmond JE, Zhao Z, Gabrieli JD. Sex differences in the neural basis of emotional memories. Proc Natl Acad Sci U S A. 2002;99:10789–94.
62. Meyer-Lindenberg A, Miletich RS, Kohn PD, Edposio G, Carson RE, Quarantelli M, et al. Reduced prefrontal activity predicts exaggerated striatal dopaminergic function in schizophrenia. Nat Neurosci. 2002;5:267–71.
63. Meyer-Lindenberg A, Kohn PD, Kolachana B, Kippenhan S, McInerney-Leo A, Nussbaum R. Midbrain dopamine and prefrontal function in humans: interaction and modulation by COMT genotype. Nat Neurosci. 2005;8:594–6.